Proceedings of the American Control Conference
San Diego, California • June 1999

STOCHASTIC RESONANCE IN AFM'S[1]

M. Basso [1], M. Dahleh [2], I. Mezić [2] and M. V. Salapaka [3]

[1] Dip. di Sistemi e Informatica, Università di Firenze, Italy.
basso@dsi.unifi.it
[2] Dept. of Mechanical and Environmental Engineering,
University of California Santa Barbara, CA 93106.
dahleh@engineering.ucsb.edu, mezic@engineering.ucsb.edu
[3] Dept. of Electrical Engineering,
Iowa State University, Ames, Iowa 50011.
murti@iastate.edu

Abstract

Stochastic resonance (SR) is an interesting phenomenon which can occur in bistable systems subject to both periodic and random forcing. This effect produces an improvement of the output signal-to-noise ratio when the input noise increases. In this paper we derive an expression for the power spectral density of a general class of systems revealing SR phenomena. This result may find useful applications in many technological contexts as, for example, in the analysis of the effects of thermal noise in Atomic Force microscopy, in order to optimize the achievable resolution for imaging.

1 Introduction

In recent years, *stochastic resonance* (SR) has attracted considerable attention in many areas of science such as physics, electronics, biology, climatology, etc. (see [1] and references therein). The term is given to a phenomenon which occurs under certain conditions in nonlinear systems where a weak periodic input signal is amplified by the presence of noise. The basic mechanism of SR can be illustrated using the simple mechanical analogy depicted in Figure 1, showing a heavily damped particle moving in a double-well potential. The following assumptions are also needed:

1. a weak periodic signal modulates the potential function, alternatively raising and lowering the wells;
2. the weak signal is not sufficient itself to cause any transition of the particle between the two wells;
3. the particle is subjected to large fluctuations generated by an external force F (noise) which induces an (irregular) switching between the wells.

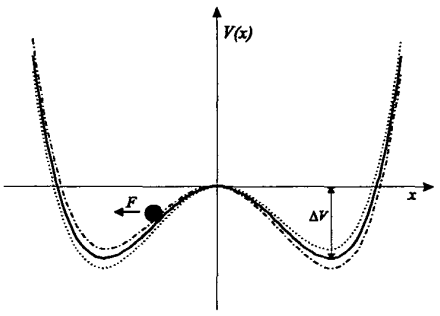

Figure 1: Sketch of a double-well potential function.

It has been proved (both experimentally and theoretically [2, 3]) that there exists an optimal level of noise which statistically enhance the regularity of the above transitions, that is, a strong frequency component arises in the power spectral density (PSD) of the particle position. A very common way to measure the SR phenomenon is through the Signal-to-Noise Ratio (SNR) of the system output (particle position in Figure 1) at the frequency of the periodic input signal. This ratio is governed by the following law [3]

$$SNR \propto \left(\frac{\epsilon}{\sigma^2}\right)^2 e^{-2\frac{\Delta V}{\sigma^2}} \quad , \tag{1}$$

where ϵ is the amplitude of the weak periodic input signal, σ^2 is the noise intensity and ΔV is the height of the potential barrier separating the wells. Indeed, the plot of the SNR as a function of the noise intensity shows the presence of a maximum. In other words, the cooperative effect induces a "non-natural" resonance phenomenon characterized by an improvement of the SNR as more noise is added to the system up to a critical value. After this value the SNR decreases when the noise level increases as it is common in most systems.

[1]Research supported by NSF grants, ECS-9733802, ECS-963820, AFOSR grant F49620-97-1-0168 and by ISU SPRIGS grant 7041747.

0-7803-4990-6/99 $10.00 © 1999 AACC

In this paper, the expression of the signal-to-noise ratio for the case of a bistable asymmetric potential is derived. This result generalizes the one previously introduced in [3] for the symmetric case and greatly extends the field of applicability of the theory. In fact, the derived expression allows one to analyse SR in a wider class of dynamical systems as the model of cantilever-sample interactions in Atomic Force Microscopy (AFM) presented in the paper.

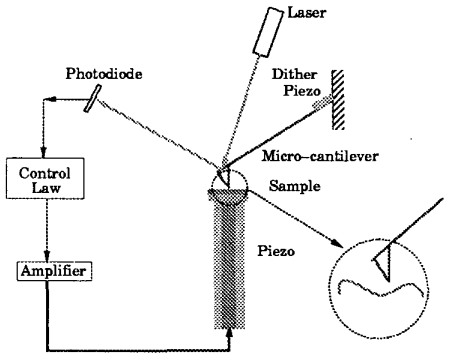

Figure 2: A schematic of an atomic force microscope.

Atomic force microscopes have revolutionized microscopy. Using this method images with sub-angstrom resolution in topography imaging have been achieved. Variants of the operating principle of the AFM have been utilized to image thermal, magnetic and electrical properties of material with resolution not available prior to the AFM [4]. Apart from its many uses, the atomic force microscope provides a system for performing experiments where interesting dynamics can be explored and studied.

A typical setup of an AFM is shown in Figure 2. It consists of a microcantilever, a sample-positioning system, a detection system and a control system. The photodiode signal is used to monitor the cantilever displacement whereas the piezo-ceramic tube is used to position the sample. A dither piezo can be used to force the cantilever. In many applications of the AFM technique the cantilever is forced sinusoidally by the dither piezo. The sample properties are inferred by monitoring the changes in the cantilever oscillations due to the sample. It will be seen later that the AFM provides a system where all the conditions mentioned earlier for the presence of stochastic resonance can be realized. Furthermore, it needs to be stressed that for such systems the assumption of a symmetric potential would be unrealistic. Noise (thermal noise) inherent in the system affects the dynamics in a significant manner and can be the limiting factor in the achievable resolution in many AFM applications (see for e.g. [5]). A study of the effect of thermal noise on the AFM dynamics is presented in [6]. Stochastic resonance can indicate a noise level so that the optimum signal-to-noise ratio is achieved, thereby optimizing the achievable resolution for imaging.

The paper is organized as follows. In Section 2 we develop the theory of stochastic resonance for a double well potential which can be asymmetric. We also find the signal-to-noise ratio of the associated stochastic process. In Section 3 we give a brief description of the cantilever-sample interaction potential and a model of the cantilever for the tapping mode dynamics of an AFM. It is shown that the model can be viewed as a particle in an asymmetric double well potential and the signal-to-noise ratio of the cantilever tip displacement is evaluated. Finally we conclude in Section 4.

2 Stochastic Resonance in a double-well potential

Consider the motion of a randomly forced particle in a bistable double-well potential modulated by an external sinusoidal signal. Its dynamics can be described by the following second order stochastic process

$$\begin{cases} \dot{x} = v \\ \dot{v} = -V'(x) - \eta v + \sigma\,\xi(t) + \epsilon\cos\omega_0 t \end{cases} \tag{2}$$

where the random variables x and v denote position and velocity of a particle of unitary mass, $V(x)$ is the potential function, η is the damping factor, $\sigma\,\xi(t)$ is a white noise with variance σ^2 and ϵ the amplitude of a sinusoidal modulation of the force. We assume the double-well potential function $V(x)$ to have local minima at $x = x_L$ and $x = x_R$ and a local maximum at $x = x_M$, such that $x_L < x_M < x_R$. In the sequel, we will denote the variables related to the left and right well with L and R, respectively.

2.1 Power Spectral Density of $x(t)$

Let us first consider the unmodulated system ($\epsilon = 0$) and suppose the particle is situated in $x = x_0$ at $t = t_0$. The "exact" solution of the stochastic process (2), i.e. the autocorrelation of the random variable $x(t)$, can only be computed numerically, except for trivial cases. This problem can be greatly simplified exploiting suitable approximated techniques developed in [7, 8, 9] and based on the computation of the conditional probability density $p(x,t) = p(x,t|x_0,t_0)$. To this aim, we define the *unmodulated transition rate* $\alpha(x_0)$ as the inverse of the mean time for the particle to cross the potential barrier at $x = x_M$. Although the transition rate depends on the initial condition x_0, it results to be quite insensitive to it. It has been proved in [9, Sec. 6.4] that up to errors of order η^{-2} (large damping), the transition rates are approximately

$$\alpha_L = \frac{\left[1+\eta^{-2}V''(x_M)\right]\sqrt{|V''(x_M)|V''(x_L)}}{2\pi\eta}\, e^{-2\eta V_L/\sigma^2}, \tag{3}$$

and

$$\alpha_R = \frac{\left[1+\eta^{-2}V''(x_M)\right]\sqrt{|V''(x_M)|V''(x_R)}}{2\pi\eta}\, e^{-2\eta V_R/\sigma^2}, \tag{4}$$

where

$$V_L = V(x_M) - V(x_L) \ , \ V_R = V(x_M) - V(x_R) \ . \quad (5)$$

We now define the time-varying potential function

$$\tilde{V}(x,t) \doteq V(x) - V(x_M) - \epsilon(x - x_L - c)\cos\omega_0 t \ , \quad (6)$$

where

$$c = \frac{x_R - x_L}{2} \ . \quad (7)$$

As it can be easily verified, the modulation of the force can be equivalently interpreted as a modulation of the potential generating the force, since this is given by

$$F(x,t) = -\tilde{V}'(x,t) = -V'(x) + \epsilon\cos\omega_0 t \ . \quad (8)$$

Assuming the period of the potential modulation small with respect to the time constants of the system dynamics, we can consider the time t as a parameter in $\tilde{V}(x,t)$ and compute the time-varying transition rates $W_L(t)$ and $W_R(t)$ similarly to (3) and (4). Now, since

$$\begin{array}{l} \tilde{V}(x_L,t) = -V_L + \epsilon c\cos\omega_0 t \ , \\ \tilde{V}(x_R,t) = -V_R - \epsilon c\cos\omega_0 t \ , \end{array} \quad (9)$$

and assuming $\epsilon c << \min(V_L, V_R)$, we can still think of $x = x_L$ and x_R as the locations of the minima of the time-varying potential. Thus, we obtain the modulated transition rates

$$\begin{array}{l} W_L(t) = \alpha_L \cdot e^{+2\beta\cos\omega_0 t} \\ W_R(t) = \alpha_R \cdot e^{-2\beta\cos\omega_0 t} \end{array} \ , \quad \beta = \frac{c\,\epsilon\,\eta}{\sigma^2} \ , \quad (10)$$

which, up to errors of order $o(\beta^2)$, can be rewritten as

$$\begin{array}{l} W_L(t) = \alpha_L \cdot [1 + 2\beta\cos\omega_0 t + 2\beta^2\cos^2\omega_0 t] \\ W_R(t) = \alpha_R \cdot [1 - 2\beta\cos\omega_0 t + 2\beta^2\cos^2\omega_0 t] \ . \end{array} \quad (11)$$

The probability n_R for a particle to be located within the right well is governed by the rate equation

$$\frac{dn_R}{dt} = W_L(t)n_L - W_R(t)n_R = W_L(t) - [W_R(t) + W_L(t)]n_R \quad (12)$$

which is a first-order linear periodic differential equation. Using (11) and dropping the higher order terms, it can be rewritten as

$$\begin{array}{l} \frac{dn_R}{dt} = \alpha_L(1 + 2\beta\cos\omega_0 t + 2\beta^2\cos^2\omega_0 t) - \\ \quad - (2\alpha + 2\gamma\beta\cos\omega_0 t + 4\alpha\beta^2\cos^2\omega_0 t)n_R \ , \end{array} \quad (13)$$

where

$$\alpha = \frac{\alpha_L + \alpha_R}{2} \ , \ \gamma = \alpha_L - \alpha_R \ . \quad (14)$$

The solution of the ODE (13) is the conditional probability of a particle to be in the right well and is given by eq. (15) (see next page) where

$$\begin{array}{l} g(t) = e^{\int_{t_0}^{t} 2\alpha + 2\gamma\beta\cos\omega_0\tau + 4\alpha\beta^2\cos^2\omega_0\tau\, d\tau} = \\ = e^{2\alpha(1+\beta^2)(t-t_0)}\left[1 + \frac{2\gamma\beta}{\omega_0}(\sin\omega_0 t - \sin\omega_0 t_0) + \right. \\ \left. + \frac{2\gamma^2\beta^2}{\omega_0^2}(\sin\omega_0 t - \sin\omega_0 t_0)^2 + \frac{\alpha\beta^2}{\omega_0}(\sin 2\omega_0 t - \sin 2\omega_0 t_0)\right] \ . \end{array} \quad (16)$$

Moreover, the initial condition $n_R(x_0, t_0)$ is equal to 1 or 0, depending whether the particle is in the right ($x_0 > x_M$) or left well ($x_0 < x_M$) at $t = t_0$, respectively.

Now, in order to compute in closed form the autocorrelation of the random variable $x(t)$ in (2), we need to generate a new stochastic variable $y(t)$ defined as

$$y = f(x) = \left\{ \begin{array}{l} 0 \ \text{if} \ x < x_M \\ 2c \ \text{if} \ x > x_M \end{array} \right. \quad (17)$$

whose probability density is given by

$$p(y,t) = n_R(t)\delta(y - 2c) + n_L(t)\delta(y) \ . \quad (18)$$

Notice that, the density functions (and the autocorrelations as a consequence) of the random variables x and $y + x_L$ get closer if the distribution $p(x,t)$ is strongly peaked at $x = x_L$ and $x = x_R$. If the latter assumption holds, the autocorrelation of $y(t)$ can be used instead.

Using expression (18), we can now derive the autocorrelation function as

$$E[y(t+\tau)y(t)|y_0,t_0] = (2c)^2 n_R(t+\tau|2c,t)n_R(t|y_0,t_0) \ . \quad (19)$$

As $t_0 \to -\infty$, $n_R(t|y_0,t_0)$ in (15) and the autocorrelation function (19) become independent of the initial state y_0. Substituting (15) into (19) and averaging on the time interval $[0, 2\pi/\omega_0]$, we get expression (20). Now, the PSD $S_{yy}(\omega)$ of the random variable $y(t)$, defined as the Fourier transform of the autocorrelation function $R(\tau)$, is computed in (21). Such expression reveals the presence of a δ-function at the signal frequency, whereas the spectrum provided by the input white noise at the system output is broadband continuous. It makes sense now to compute the signal-to-noise ratio of the random variable $y(t)$ as the relative increment of the PSD at the frequency ω_0 of the signal input

$$SNR \doteq \frac{S_{yy}(\omega_0) - \lim\limits_{\omega\to\omega_0} S_{yy}(\omega)}{\lim\limits_{\omega\to\omega_0} S_{yy}(\omega)} \quad (22)$$

which can be reduced to the expression

$$SNR = \frac{4\pi c^2\epsilon^2\eta^2\delta(0)}{\sigma^4(\alpha_L^{-1} + \alpha_R^{-1})} + o(\beta^2) \ . \quad (23)$$

As expected, stochastic resonance is characterized by the presence of a maximum in the SNR. For symmetric potential functions, this is achieved at a noise intensity

$$\sigma^2_{\max} = \eta V_L = \eta V_R \ , \quad (24)$$

while it can be computed numerically in the asymmetric case.

3 Tapping mode dynamics in an AFM

Consider the AFM system depicted in Figure 2, where the cantilever is subjected to a small sinusoidal force and random white noise through a dither piezo. The

$$n_R(t|x_0,t_0) = \left[n_R(x_0,t_0) + \int_{t_0}^{t} \alpha_L(1+2\beta\cos\omega_0 t' + 2\beta^2\cos^2\omega_0 t')g(t')dt'\right]g^{-1}(t) = \left[n_R(x_0,t_0)+\right.$$
$$+ \tfrac{\alpha_L}{2\alpha}\left(e^{2\alpha(1+\beta^2)(t-t_0)}-1\right)\left(1-2\tfrac{\gamma\beta}{\omega_0}\sin\omega_0 t_0 + 2\tfrac{\gamma^2\beta^2}{\omega_0^2}\sin^2\omega_0 t_0 + \tfrac{\gamma^2\beta^2}{\omega_0^2} - \tfrac{\alpha\beta^2}{\omega_0}\sin 2\omega_0 t_0\right)+$$
$$+ \tfrac{\alpha_L}{\omega_0^2+4\alpha^2}\left(e^{2\alpha(1+\beta^2)(t-t_0)}\sin\omega_0 t - \sin\omega_0 t_0\right)\left(\tfrac{4\alpha\gamma\beta}{\omega_0} - \tfrac{8\alpha\gamma^2\beta^2}{\omega_0^2}\sin\omega_0 t_0 + 2\omega_0\beta - 4\gamma\beta^2\sin\omega_0 t_0\right)+ \quad (15)$$
$$+ \tfrac{\alpha_L}{\omega_0^2+4\alpha^2}\left(e^{2\alpha(1+\beta^2)(t-t_0)}\cos\omega_0 t - \cos\omega_0 t_0\right)\left(4\alpha\beta - \tfrac{8\alpha\gamma\beta^2}{\omega_0}\sin\omega_0 t_0 - 2\gamma\beta + \tfrac{4\gamma^2\beta^2}{\omega_0}\sin\omega_0 t_0\right)+$$
$$+ \tfrac{2\alpha_L}{4\omega_0^2+4\alpha^2}\left(e^{2\alpha(1+\beta^2)(t-t_0)}\sin 2\omega_0 t - \sin 2\omega_0 t_0\right)\left(\tfrac{\alpha^2\beta^2}{\omega_0} + \tfrac{2\alpha\gamma\beta^2}{\omega_0} + \omega_0\beta^2 - \tfrac{\gamma^2\beta^2}{\omega_0}\right)-$$
$$\left.- \tfrac{2\alpha_L}{4\omega_0^2+4\alpha^2}\left(e^{2\alpha(1+\beta^2)(t-t_0)}\cos 2\omega_0 t - \cos 2\omega_0 t_0\right)\left(2\gamma\beta^2 + \tfrac{\alpha\gamma^2\beta^2}{\omega_0^2}\right)\right]g^{-1}(t) + o(\beta^2)$$

$$R(\tau) = < E[y(t+\tau)y(t)] >_t = c^2\, e^{-2\alpha(1+\beta^2)|\tau|}\left[1 - \left(\tfrac{\gamma}{2\alpha}\right)^2 - \tfrac{2\alpha_L\gamma^3\beta^2}{\alpha^2\omega_0^2} - \tfrac{8\alpha_L^2(\alpha-\gamma)\beta^2}{\alpha(4\alpha^2+\omega_0^2)} + \tfrac{8\alpha_L^2\gamma^2\beta^2}{\omega_0^2(4\alpha^2+\omega_0^2)}+\right.$$
$$+ \tfrac{(8\alpha\alpha_L^2\omega_0^2\gamma+8\alpha^2\alpha_L\gamma^3-8\alpha^2\alpha_L^2\gamma^2-2\alpha_L^2\omega_0^2\gamma^2-8\alpha^2\alpha_L\omega_0^2\gamma)\beta^2}{\alpha^2\omega_0^2(4\alpha^2+\omega_0^2)}\cos\omega_0\tau + \tfrac{8\alpha_L\alpha_R\gamma^2\beta^2}{\alpha\omega_0(4\alpha^2+\omega_0^2)}\sin\omega_0|\tau|\Big] + \quad (20)$$
$$\left.+ c^2\left[\left(\tfrac{\alpha_L}{\alpha}\right)^2 - \tfrac{8\alpha_L^2\alpha_R\gamma\beta^2}{\alpha^2(4\alpha^2+\omega_0^2)} + \tfrac{8\alpha_L^2\alpha_R^2\beta^2}{\alpha^2(4\alpha^2+\omega_0^2)}\cos\omega_0\tau\right] + o(\beta^2)\right.$$

$$S_{yy}(\omega) = \int_{-\infty}^{\infty} R(\tau)e^{-j\omega\tau}d\tau = \left[1 - \left(\tfrac{\gamma}{2\alpha}\right)^2 - \tfrac{2\alpha_L\gamma^3\beta^2}{\alpha^2\omega_0^2} - \tfrac{8\alpha_L^2(\alpha-\gamma)\beta^2}{\alpha(4\alpha^2+\omega_0^2)} + \tfrac{8\alpha_L^2\gamma^2\beta^2}{\omega_0^2(4\alpha^2+\omega_0^2)}\right]\tfrac{4c^2\alpha}{4\alpha^2+\omega^2}+$$
$$+ \gamma\beta^2\left[\tfrac{8\alpha\alpha_L^2\omega_0^2+8\alpha^2\alpha_L\gamma^2-8\alpha^2\alpha_L^2\gamma-2\alpha_L^2\omega_0^2\gamma-8\alpha^2\alpha_L\omega_0^2}{\alpha^2\omega_0^2(4\alpha^2+\omega_0^2)}\right]\cdot\left[\tfrac{2c^2\alpha}{4\alpha^2+(\omega-\omega_0)^2} + \tfrac{2c^2\alpha}{4\alpha^2+(\omega+\omega_0)^2}\right]+$$
$$+ \gamma^2\beta^2\left[\tfrac{8\alpha_L\alpha_R}{\alpha\omega_0(4\alpha^2+\omega_0^2)}\right]\cdot\left[\tfrac{c^2(\omega_0-\omega)}{4\alpha^2+(\omega-\omega_0)^2} + \tfrac{c^2(\omega_0+\omega)}{4\alpha^2+(\omega+\omega_0)^2}\right] + 2\pi c^2\delta(\omega)\left[\left(\tfrac{\alpha_L}{\alpha}\right)^2 - \tfrac{8\alpha_L^2\alpha_R\gamma\beta^2}{\alpha^2(4\alpha^2+\omega_0^2)}\right]+ \quad (21)$$
$$+ \pi c^2\left[\delta(\omega-\omega_0)+\delta(\omega+\omega_0)\right]\cdot\tfrac{8\alpha_L^2\alpha_R^2\beta^2}{\alpha^2(4\alpha^2+\omega_0^2)} + o(\beta^2)$$

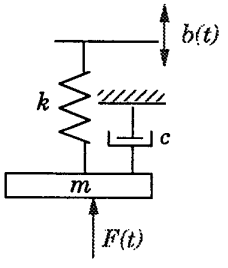

Figure 3: Model of the cantilever

dynamical equation for the displacement x of the cantilever (see Figure 3) is given by

$$m\ddot{x} + c\dot{x} + kx = F(t) + kb(t), \quad (25)$$

where $b(t)$ is the base motion of the cantilever and

$$F = -\frac{m\,d}{(x+Z)^2} + \frac{m\,d\,\Sigma^6}{30(x+Z)^8}\,, \quad (26)$$

indicates long range attractive forces and short range strong repulsive forces acting on the cantilever due to a sample at distance Z. Σ and d are parameter that depend on the nature of the tip and the sample. This system can be recast in the form (2) using the bistable potential energy

$$V(x) = \frac{k_1}{2}x^2 - \frac{d}{(x+Z)} + \frac{\Sigma^6 d}{210(x+Z)^7}\,, \quad (27)$$

where $k_1 = \frac{k}{m}$ represents the natural frequency of the cantilever and $\eta = \frac{c}{m}$. For example, setting the following parameters

$$k_1 = 40\ ,\ d = 0.26\ ,\ \Sigma = 0.05\ ,\ \eta = 30\ ,$$
$$\epsilon = 1\ ,\ \omega_0 = 0.1\pi\ ,\ Z = 0.5\ , \quad (28)$$

yields the potential function reported in Figure 4. Notice that the above described potential is double-welled, hence the theory developed in Section 2 can be applied to the cantilever-sample interaction dynamics.

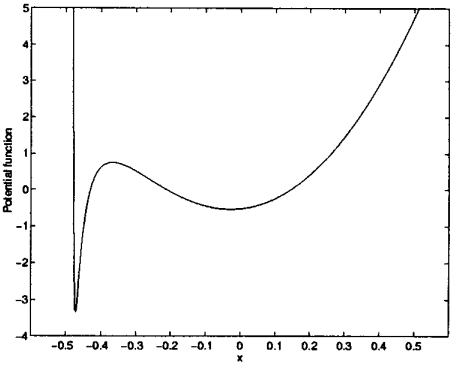

Figure 4: Potential function of eq.(27).

The analysis of the signal-to-noise ratio of the position x of the tip using expression (23) yields the diagram shown in Figure 5, where the SNR is reported as a function of the noise intensity σ^2 and the parameter Z. The theoretical PSD and SNR computed via (21) and (23) are in good agreement with the results given by integrating system (2) with (27) and reported in Figures 6 and 7. As can be seen in Figure 5, the SNR has maximum at a nonzero value of the noise variance for any fixed Z. This indicates that adding noise can be beneficial in achieving a higher SNR, thereby leading to improvements in achievable resolution. Also, the

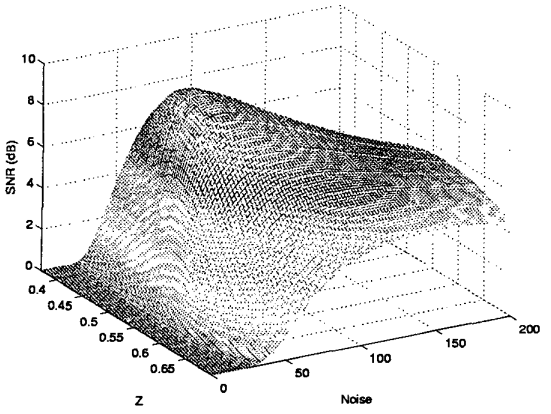

Figure 5: Signal-to-noise ratio of the AFM system as a function of σ^2 and Z.

plot indicates that the SNR for a fixed variance of the noise has a maximum at a fixed value of the parameter Z. This suggests that there is an optimal separation between the cantilever and the sample that needs to be maintained for a fixed noise source (which could be the thermal noise). These conclusions suggest experiments to evaluate the benefits of stochastic resonance. The parameter Z can be changed by using the positioning piezo (see Figure 2), whereas the noise can be added by using the dither piezo in the AFM setup. The output of the cantilever deflection can then be monitored by a signal analyzer. These experiments are a part of the ongoing research.

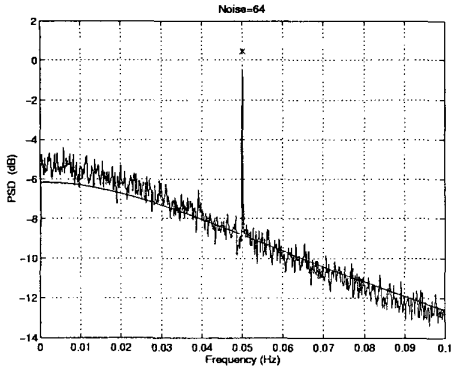

Figure 6: AFM system: Comparison of the predicted PSD (solid line plus the 'x' mark) with simulations at the SNR maximum ($\sigma^2 = 64$, $Z = 0.5$).

4 Conclusions

The paper has analyzed stochastic resonance effects in a general class of (asymmetric) bistable systems affected by noise. The obtained results have made possible to compute the output power spectral density as a function of the system parameters, thus making clear the

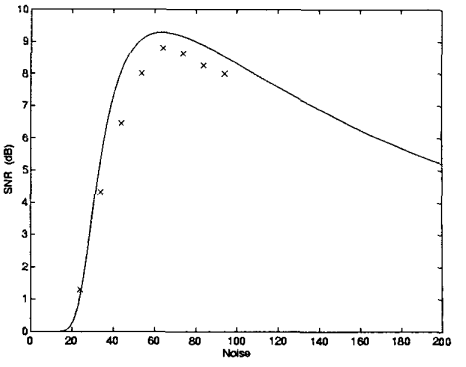

Figure 7: AFM system: Comparison of the predicted SNR with simulations ('x' marks) at $Z = 0.5$.

relevance of stochastic resonance in technological applications. In this context, the model of a tapping mode Atomic Force microscope has been considered. Its analysis has proved that conditions for the presence of stochastic resonance can be realized. The theoretical result has been confirmed by numerical simulations, while experiments will be part of the ongoing research.

References

[1] Wiesenfeld, K. and Moss, F., "Stochastic resonance and the benefits of noise: From ice ages to crayfish and SQUIDs", *Nature*, **373**, pp. 33-36, 1995.

[2] Bulsara, A.R., and Gammaitoni, L., "Tuning in to noise", *Physics Today*, pp. 39-45, March 1996.

[3] McNamara, B., and Wiesenfeld, K., "Theory of stochastic resonance", *Physical Review A*, **39**, pp. 4854-4869, 1989.

[4] Sarid, D., *Scanning Force Microscopy*, Oxford University Press, New York, 1994.

[5] Rugar, D. and Zuger, O. and Hoen, S. and Yannoni, C. S. and Vieth, H. M. and Kendrick, R. D.", "Force detection and nuclear magnetic resonance, Science, **264**, pp. 1560-1563, 1994.

[6] Salapaka, M.V., Bergh, H.S., Lai, J., Majumdar, A., and McFarland, E., "Multimode noise analysis of cantilevers for scanning probe microscopy", Journal of Applied Physics, **81**, pp. 2480-2487, 1997.

[7] Caroli, B., Caroli, C., Roulet, B., and Saint-James, D., "On fluctuations and relaxation in systems described by a one-dimensional Fokker-Plank equation with a time-dependent potential", *Physica A*, **108**, pp. 233-256, 1981.

[8] Kramers, H.A., "Brownian motion in a field of force and the diffusion model of chemical reactions", *Physica*, **7**, pp. 284-304, 1940.

[9] Gardiner, C.W., *Handbook of Stochastic Methods for Physics, Chemistry, and the Natural Sciences*, Springer-Verlag, Berlin, 1983.